Antibody selection procedure for cardiac troponin I ELISA development using quantitative mass spectrometric immunoassays

Lowenthal MS[1]*, Gasca-Aragon H[1], Schiel JE[1], Dodder NG[2], Bunk DM[1]
[1] Analytical Chemistry Division, National Institute of Standards and Technology, Gaithersburg, MD 20899-8392, USA
[2] Chemistry Division, Southern California Coastal Water Research Project, Costa Mesa, CA 92626, USA
* corresponding author, email: mark.lowenthal@nist.gov

Abstract

A mass spectrometry-based antibody selection procedure targeting human cardiac troponin I (cTnI) was established for the purpose of developing a well-characterized secondary reference measurement procedure. A panel of six monoclonal antibodies (mAb) was evaluated based on relative binding affinity to cTnI as determined by isotope-dilution liquid chromatography-tandem mass spectrometry (ID LC-MS/MS) quantification following immunoprecipitation using a magnetic bead solid support. Dissociation constants (K_d) were determined for each mAb-cTnI pair using non-linear regression curve fitting over the diagnostic range 0.2-0.8 for bound [mAb-cTnI] / total [mAb]. Quantification of all three cTn subunits, and of each antibody isotype, was based on the use of stable isotope-labeled peptide analogs as internal standards. The mAb, 19C7, was determined to have the lowest K_d constant among the pre-screened antibody panel using the NIST Standard Reference Material (SRM) 2921 – Human Cardiac Troponin Complex. ID LC-MS^2 is shown to be capable of quantitatively differentiating certain mAbs based on their relative binding affinities. Selection of the optimal 'capture' mAb for cTnI will be applied towards the development of a well-characterized assay based on an ELISA measurement procedure.

Introduction

Human cardiac troponin (cTn) is both a sensitive and specific diagnostic marker for heart muscle damage [1-4]. This protein complex, consisting of three regulatory subunits (designated C, T, and I), is integral to muscle contraction and is released from tissue into the bloodstream as a result of damage to cardiac muscle. Routinely, cTn concentrations are measured in serum using commercially available immunoassay kits for patients presenting with chest pains or acute coronary syndrome in order to differentiate stable angina from a suspected myocardial infarction [5]. Additionally, elevated serum cTn concentrations are prognostically important to many of the conditions in which they are used for diagnosis [6]. Due to patent regulations, a single manufacturer produces a cTnT immunoassay kit, whereas many different immunoassay platforms are commercially available targeting cTnI. Unfortunately, measurements using α-cTnI commercial assays suffer from poor standardization, high clinical variability, and poor diagnostic specificity [7;8]. Efforts by the International Federation of Clinical Chemistry (IFCC) to standardize clinical cTn measurements using a proposed secondary reference material (cTnI-positive human serum pool) are dependent on the establishment of a reproducible and repeatable reference measurement procedure based on well-characterized measurements of cTnI.

In attempt to standardize cTn measurements, it is important to note that the microheterogeneity of cTn in serum caused by proteolytic degradation may lead to the appearance of a diversity of measurands with varying stabilities [9]. Katrukha et al (1998) has determined that any serum-based cTnI assay should incorporate antibodies targeting the stable region of cTnI between residues 30 and 110 – although there is no inclusive consensus of what is the stable region of cTnI. In any case, the panel of mAbs selected for this assessment was based on previous western blotting and Luminex data performed by the IFCC WG-TNI [10]. Other mAbs targeting the stable region of cTnI were initially rejected due to performance issues such as only binding free cTnI, cross-reactivity with skeletal muscle TnI, and low avidity [5;11]. Among those mAbs included in the current assessment, three (3C7, 19C7, and 560) bind at least partially to the cTnI 'stable region' from residues 30-110. However, both this manuscript, and that from the IFCC WG-TNI determined optimal 'capture' mAbs based on experimental approaches using NIST SRM 2921 (intact cTn complex) and not serum-proteolyzed cTn. Therefore, a comparison among this pre-selected mAb panel remains significant as a generally applicable mass spectrometry-based methodology for antibody selection.

Antibody selection for immunoassay measurement procedures is routinely performed using high-throughput, yet potentially inaccurate approaches, such as ELISAs. These techniques are inherently susceptible to interferences and biases as a result of the indirect relationship between what is being measured (a fluorescence signal of an enzyme reaction) and the protein measurand of interest (cTn). Consequently, without rigorous examination of the chemistry involved, ELISAs and similar approaches lack the metrological traceability that is a necessary component of a reference measurement procedure. Ultimately, a measurement procedure based on mass spectrometry is desired for use in value assignment of reference materials. Here, we demonstrate an approach to pre-select mAbs targeted for a reference measurement procedure based on analytical scrutiny of the chemical interaction steps in a measurement cascade. This metrological traceability will eventually be applied to an ELISA measurement process. In contrast, for an ELISA that is developed only through signal optimization, the possibility of potential biases may remain hidden.

Future selection of antibody pairs will be approached sequentially – first the selection of the 'capture' antibody, followed by selection of the optimal 'detection' mAb. Here, we describe details of the first step and allude to methodology for selection of the 'detection' mAb which will follow in later work. This approach is being developed with the consideration of being universally applicable for mAb-antigen interactions. The method uses ID LC-MS/MS based on multiple-reaction monitoring (MRM) of peptide fragmentation transitions. Following immunoprecipitation of the antigen (cTn complex) and enzymatic digestion, an equimolar mixture of isotopically-labeled synthetic peptides corresponding to each subunit of the cTn complex was used as an internal standard. Similarly, labeled peptides corresponding to the constant regions of each mAb (IgG) isotype were quantified to validate consistency of the concentration of magnetic bead-bound antibody used for all points in a saturation curve. Matrix-matched calibration curves were used to determine recovery of antigen from each immunoprecipitation, and a

saturation curve was created using non-linear regression analysis for the $[\text{mAb-cTn}]_{bound}$ vs. $[\text{cTn}]_{free}$ data. Finally, K_d constants were assigned to each cTnI-mAb_{bead} interaction, and the optimal 'capture' mAb was determined by evaluation of relative K_d constants for each peptide transition.

Experimental

Materials

Human, cardiac troponin complex was obtained as Standard Reference Material (SRM) 2921 from the National Institute of Standards and Technology (NIST) and is described in detail in a Certificate of Analysis[12]. All other reagents used in this analysis were obtained from commercial sources. Isotopically-labeled ^{15}N and/or ^{13}C synthetic peptides of each troponin subunit and all IgG isotypes and their unlabeled analogs were purchased through AnaSpec, Inc (San Jose, CA) and are detailed in Table 1. α-cTnI monoclonal antibodies were purchased through HyTest Ltd (Turko, Finland). α-GAPDH mAb (used for negative control) was purchased through Calbiochem (San Diego, CA). Dynabead MyOne Tosyl-activated magnetic beads were purchased through Invitrogen Corp. (Oslo, Norway). Rapigest SF Surfactant was purchased through Waters Corp. (Milford, MA). Sequencing grade modified porcine trypsin was purchased through Promega (Madison, WI). Bovine serum albumin (BSA), sodium borate, trifluoroacetic acid, tween-20, tris, sodium chloride, dithiolthreitol (DTT), iodoacetamide (IAM), sodium azide, and hydrochloric acid (HCl) were purchased through Sigma-Aldrich. High purity LC-MS grade water/formic acid and acetonitrile/formic acid were purchased from Honeywell – Burdick and Jackson.

Preparation of mAb – magnetic bead conjugates

Each of six α-cTnI monoclonal antibodies and one α-GAPDH mAb (negative control) was separately immobilized to a solid magnetic bead support under optimized conditions according to a modification of the manufacturer's (Dynal) instructions for use. Briefly, mAb-bead conjugates were formed by covalent interaction of activated hydroxyl groups on the bead surface to amino groups located [ideally] within the IgG constant region. Antibodies (125 µg) were activated for 15 minutes at room temperature by addition of 0.0025 % TFA and neutralized in 0.1 mol/L Na_3BO_3 buffer (pH 9.5). A ratio of 40 µg mAb / mg of Dynabeads was used for optimal coating. 3.12 mg of prewashed (3X in borate buffer) magnetic beads were added to the activated mAbs. Bead concentration during coating was ≈ 40 mg/mL. mAbs were crosslinked to the magnetic beads with addition of 3 mol/L ammonium sulfate (1 mol/L final concentration, in 0.1 mol/L Na_3BO_3 buffer, pH 9.5). The mixture was rotated end-over-end for 96 hours at 25 ^oC. Next, the supernatant was discarded and the mAb-bead complex was incubated in PBS containing 0.5 % (w/v) BSA / 0.05 % (v/v) tween-20 for 16 hours at 37 ^oC to block uncoated bead surfaces and limit non-specific binding. Finally, the mAb-bead conjugates were washed 3X in PBS containing 0.1 % (w/v) BSA / 0.05 % tween 20 / 0.02 % (w/v) sodium azide (preservative) and stored at 4 ^oC. Each mAb-bead complex was prepared to a final [mAb] of ≈ 2 µmol/L based on stoichiometric crosslinking.

Immunoprecipitation (IP) of cTn

Human cTn complex from NIST SRM 2921 was thawed at room temperature for 15 minutes, diluted in 120 – 130 µL of 0.2 % (w/v) BSA, and added at eight different levels (≈ 2.5, 7.8, 13.3, 18.9, 24.5, 30.0, 35.5, 41.4 pmol) to a constant molar addition of mAb-bead complex (≈ 40 pmol mAb) corresponding to cTn concentrations during IP of ≈ 0.016, 0.049, 0.082, 0.12, 0.15, 0.18, 0.22, to 0.25 µmol/L. These eight samples were replicated for each of six α-cTnI mAbs (labeled as MF4, M18, 3C7, 19C7, 560, and 267) and one α-GAPDH mAb used as a negative control. The design was intended to cover the entire optimal IP range 0.2-0.8 for $bound_{[mAb\text{-}cTnI]}$ / $total_{[mAb]}$ at eight discrete points along the predicted K_d curve. Samples were rotated end-over-end for three hours at 25 ^{o}C to ensure equilibrium. mAb-bead—antigen complexes were isolated using a magnet (Dynal Magnetic Particle Concentrator) and the supernatant was removed and discarded prior to being washed twice with ≈ 400 µL TBST (0.1 % (v/v) tween-20, 20 mmol/L tris, 137 mmol/L NaCl) containing 0.1 % (w/v) BSA, followed by a single wash of ≈ 400 µL 0.1 % (w/v) BSA in water. Supernatant was removed and discarded prior to digestion.

The washed mAb-bead—antigen complexes were reconstituted in 40 µL 0.1% Rapigest surfactant in 100 mmol/L NH_4HCO_3 and boiled for two minutes. Disulfide linkages in the denatured proteins were reduced by the addition of ≈ 5 µL of 50 mmol/L DTT and shaken at 60 ^{o}C for 30 minutes. Cysteine residues were alkylated in the dark for 30 minutes using iodoacetamide at a final concentration of 15 mmol/L. Samples were tryptically digested without bead removal using a 40:1 total protein : trypsin ratio for 16 hours at 37 ^{o}C with shaking. Rapigest was cleaved by addition of 0.1 mol/L HCl and removed by centrifugation at 4 ^{o}C. Finally, eight isotopically-labeled peptides corresponding to each subunit of the cTn complex and to each IgG (mAb) isotype were spiked into the sample at a constant concentration (≈ 0.18 µmol/L and 0.36 µmol/L, respectively) to serve as an internal standard for isotope dilution quantification. Final unlabeled : labeled molar mass ratios ranged from ≈ 0.15 – 2.5 among the eight points along the saturation curve (see Supplementary Table 1). Matrix-matched calibration solutions were prepared from NIST SRM 2921 at six discrete concentrations ranging from ≈ 0.023 – 0.41 µmol/L corresponding to unlabeled : labeled mass ratios of ≈ 0.12 – 2.65 following the addition of internal standard. Calibration solutions were carried through the identical experimental procedures as the samples using an equimolar mixture of all mAbs and by omitting the wash steps to ensure complete recovery. Similarly, parallel experiments designed to test reproducibility associated with the preparation of the mAb-bead complex were performed, and will be discussed in the Results section.

Isotope-dilution liquid chromatography-tandem mass spectrometry (ID LC-MS/MS) analysis

Liquid chromatographic separation was achieved using a Zorbax (Agilent) SB-C_{18} reversed-phase analytical column (2.1 x 150 mm, 3.5 µm particles) at a flow rate of 200 µL/min. Peptide elution was accomplished using an increasing linear gradient of organic/aqueous solvent (ACN/H_2O) up to 50 % B over 33 minutes, followed by a column wash and re-equilibration. Mobile phases A and B consisted of 0.1 % (v/v) formic acid in H_2O and ACN, respectively. Column temperature was maintained at 35 ^{o}C; autosampler plate temperature control was set at 5 ^{o}C. Blank injections were

monitored for sample carry-over. An Agilent 1200 LC system (Santa Clara, CA) was coupled in-line with an Applied Biosystems API 5000 triple quadrupole mass spectrometer (Foster City, CA) equipped with a standard micro-flow source. Ions were detected using a scheduled multiple-reaction monitoring (MRM) method in positive ion mode with a target scan time of 1 second and a MRM detection window of 30 seconds. Two fragmentation transitions were monitored per peptide from a total of five cTn peptides (three from cTnI, one from cTnT, and one from cTnC) and three IgG peptide isotypes (one each for IgG_1 IgG_{2a}, and IgG_{2b}) (refer to Table 1) for both the isotopically-labeled, and -unlabeled isoforms. The optimum peptides were selected using a previously described procedure [13] and the OrgMassSpecR computer program [14]. Optimized source and fragmentation parameters (declustering potential, entrance potential, collision energy, and collision cell exit potential) were selected independently for all peptide transitions by monitoring MS-response over a broad range and noting maximum signal intensity (see Table 2). Isotopically-labeled peptide analogs were additionally infused to validate the optimization results and to verify negligible isotope effect. During data acquisition, all source and fragmentation parameters were set identically for unlabeled/labeled pairs: collision gas = 3.4×10^4 Pa (5 psi), unit resolution in Q1 & Q3, curtain gas (CUR) = 4.1×10^5 Pa (60 psi), intensity threshold = 0, ion source gas 1 (GS1) = 2.8×10^5 Pa (40 psi), settling time = 5 ms, ion source gas 2 (GS2) = 2.8×10^5 Pa (40 psi), pause between mass ranges = 5 ms, ion spray voltage (IS) = 5000 V, x-axis spray position (vert.) = 0 mm, capillary temperature (TEM) = 500°C, y-axis spray position (horiz.) = 7 mm, target scan time = 1.3 s, interface heater = ON, and MRM detection window = 60 s. Data acquisition and peak integration was performed using Analyst v1.5 software (Applied Biosystems). Peaks were identified manually and were automatically selected by the Analyst Quantitation Wizard; peak areas were integrated by Analyst using a bunching factor = 1, number of smooths = 0, and all other parameters set to default values. All peak integrations were visually inspected and manually integrated when necessary.

Non-linear curve fitting and error determination

Troponin concentrations as determined by ID LC-MS/MS analyses were fitted to non-linear curves on a two-dimensional plot consisting of parameters of 'bound Ab-Ag' versus 'free Ag'. The model [15;16] that relates the free troponin and the bound troponin measurements is:

$[\mathrm{AbAg}] = \dfrac{[\mathrm{R_T}][\mathrm{Ag}]}{K_d + [\mathrm{Ag}]}$. (See the derivation in Results and Discussion below). Let

$$Y_i = f(x_i, \gamma) + Z_i$$

where

$x_i = \begin{bmatrix} x_{i1} \\ \vdots \\ x_{iq} \end{bmatrix}$ are the values of the independent variable, $\gamma = \begin{bmatrix} \gamma_0 \\ \vdots \\ \gamma_{p-1} \end{bmatrix}$ are p unknown parameters, $f(x_i, \gamma)$ is the nonlinear response function, and Z_i are the error terms assumed

to be independent and normally distributed. The Gauss-Newton method was used in order to find the least squares estimates of the parameters, which uses a Taylor series expansion of the nonlinear response function $f(X,\gamma)$, by providing initial values for the parameters $\gamma_k^{(0)}$ and iterating for updated estimates until convergence was obtained. For

$$f(x_i,\gamma) \approx f(x_i,\gamma^{(0)}) + \sum_{k=1}^{p-1}\left[\frac{\partial f(X_i,\gamma)}{\partial \gamma_k}\right]\Big|_{\gamma=\gamma^{(0)}}(\gamma_k - \gamma_k^{(0)})$$

at the t^{th} iteration, we can rewrite the function as:

$$f(\gamma^{(t+1)}) \approx f(\gamma^{(t)}) + V^{(t)}\Delta^{(t)}$$

where $V^{(t)}$ is the NxP derivative matrix at iteration t, with elements $\left[\frac{\partial f(X_i,\gamma)}{\partial \gamma_k}\right]\Big|_{\gamma=\gamma^{(t)}}$ and $\Delta^{(t)} = \gamma_k - \gamma_k^{(t)}$. We then calculate the increment in the parameters $\delta^{(t)}$ to minimize the approximate residual sum of squares: $SSE = \sum_{i=1}^{n} Z_i^2 = \sum_{i=1}^{n}(Y_i - f(X_i,\gamma))^2$ by using the QR decomposition of $V^{(t)}$:

$$V^{(t)} = Q^{(t)}R^{(t)} = Q_1^{(t)}R_1^{(t)},$$

$$\gamma^{(t+1)} = \gamma^{(t)} + \delta^{(t)} = \gamma^{(t)} + (R_1^{(t)})^{-1}Q_1^{(t)T}Z^{(t)}$$

where $\gamma^{(t+1)}$ is a better parameter estimate. When convergence is obtained, the final estimates are denoted by $\hat{\gamma}, \hat{Q}_1, \hat{R}_1, \widehat{SSE}$. Approximate confidence regions for a nonlinear model are defined as:

$$\left\{\gamma = \hat{\gamma} + \sqrt{P\, s^2 F(P, N-P; \alpha)}\hat{R}_1^{-1}d \mid \|d\| = 1\right\}$$

and the $1-\alpha$ approximate inference band is

$$f(x_i,\gamma) = f(x_i,\hat{\gamma}) \pm s\left\|v^T\hat{R}_1^{-1}\right\|\sqrt{P\, s^2 F(P, N-P; \alpha)}$$

where

$$s^2 = \frac{\widehat{SSE}}{N-P}, \qquad v^T = \left[\frac{\partial f(X,\gamma)}{\partial \gamma_k}\right]\Big|_{\hat{\gamma}}$$

and X is a vector of points necessary to estimate the confidence band. When multiple data sets were available the parameters were estimated simultaneously by extending the model accordingly, to illustrate this, we detail the model for two data sets:

$$[\mathrm{AbAg}] = \frac{[\mathrm{R_T} + \Delta\mathrm{R_T} \times g][\mathrm{Ag}]}{K_d + \Delta K_d \times g + [\mathrm{Ag}]}$$

Where g can take the values 0 or 1 indicating to which dataset the data belongs, and we proceed to test for the additional parameters $\Delta R_t, \Delta K_d$ to be non zero. In order to get confidence intervals within the parameter space we used the nonlinear solution and applied a parametric bootstrap technique to estimate the maximum likelihood of the parameters and a 95% confidence interval. The nls function available in the R language within the stats package was used [17]. The R script used for this work is included in the Supplementary Data.

Results and Discussion

Standardization of a reference immunoassay measurement procedure for cTn is of vital importance for the clinical community. Building on the success of the International Federation of Clinical Chemistry's cTnI working group (IFCC WG-TNI), we have developed a method to quantitatively select among monoclonal antibodies from a panel of high-performing, pre-screened α-cTnI mAbs based on their relative binding affinities using ID LC-MS/MS.

The amino acid sequence of cTnI is shown in Figure 1. Those regions against which each mAb was raised are highlighted, as are the amino acid sequences for which isotopically labeled peptides were synthesized for use as internal standards. cTnI is known to have multiple phosphorylation sites [19], most notable are those at Ser-23 and Ser-24 which have widely accepted functional significance in the control of cardiac contractility [20;21], and which are located on a unique N-terminal extension of the cTnI variant not found in skeletal TnI [22;23]. A representative MRM trace is provided in Figure 2. Each experiment monitored two unique precursor-to-product ion transitions for each of five cTn peptides and three IgG peptides, for both the labeled and unlabeled peptide analogs. Table 2 lists the instrumental parameters used to monitor each MRM transition. Three peptides originating from the cTnI subunit were quantified along with one peptide each from the cTnT and cTnC subunits. Although the cTnI subunit contains the binding epitope for all mAbs used in this study and for any corresponding ELISA, we also quantified peptides from the T and C subunits to validate the stability of the intact cTn complex during the experimental procedure. These peptides exhibit relative agreement to cTnI peptides (see below). In all cases, signal was detected from IgG peptide transitions specific for the antibody isotype used in that assay; the isotopically-labeled IgG peptide transitions were detected in all assays. IgG peptides were previously selected from the antibody constant region by digesting a representative IgG isotype, and measuring a set of theoretical MRM transitions, as described for the cTn peptide selection (see Supplementary Figure 1 and Supplementary Table 2).

In this work, we treat the thermodynamics of Ab-Ag binding as a reversible bimolecular reaction with a K_a representing the affinity of the Ag for the Ab-bead conjugate, and $K_d = K_a^{-1}$. For the equilibrium reaction Ab + Ag $\Leftrightarrow$ AbAg,

$$K_d = \frac{[\mathrm{Ab}][\mathrm{Ag}]}{[\mathrm{AbAg}]} = \frac{1}{K_a} \qquad \textbf{[1]}$$

The mass action law [1] can be rewritten as:

$$[\mathrm{AbAg}] = K_a[\mathrm{Ab}][\mathrm{Ag}] = \frac{([\mathrm{Ab_{tot}}] - [\mathrm{AbAg}])[\mathrm{Ag}]}{K_d} \qquad \textbf{[2]}$$

or

$$[\mathrm{AbAg}] = \frac{[\mathrm{Ab_{tot}}][\mathrm{Ag}]}{K_d + [\mathrm{Ag}]} \qquad \textbf{[3]}$$

where Ab_{tot} = [Ab] + [AbAg], and when Ab_{tot} is written as equal to B_{max} the equilibrium data can be plotted as:

$$y = \frac{(\mathrm{B_{max}})(x)}{K_d + x}, \qquad \textbf{[4]}$$

so that the concentration of [AbAg] complex increases linearly with increasing [antigen] at low [antigen], and the slope tapers off at higher [antigen] to reach an asymptotic plateau at B_{max} as all Ab is saturated. The dissociation constant K_d has units of mol/L. For a high-affinity Ab-Ag equilibrium, a $K_d \approx 10^{-9}$ mol/L is typical [24], being, as expected, approximately an order of magnitude lower than the dissociation constants determined for the best binding mAbs in our α-cTnI panel. It is suggested [25-27] that immobilization of an antibody on a solid surface – in this case on magnetic beads – can affect the binding constants for an Ab-Ag equilibrium. Therefore, what is being measured here is the immobilized non-intrinsic binding affinity – which also mimics the immobilization approach that is used in developing an ELISA assay where mAbs are bound to solid supports via reactive amine groups.

Calibration curves were developed for each peptide transition and exhibited linear regression R^2 values > 0.99 (see Supplementary Figure 2). Non-linear saturation curve data was determined by extrapolation through linear calibration curves. K_d constants were determined as [cTn_{free}] concentration at one-half of the maximum [$bound_{cTn}$] concentration (½ B_{max}) using an iterative fit to all nonlinear curve data. All data points are corrected for by subtracting the binding to a non-specific antibody (α-GAPDH) measured at each of the eight antigen concentrations. Non-specific binding of cTn to the bead surface and/or to the F_C region of the antibody estimated from α-GAPDH assays was typically negligible suggesting that our washing protocols were sufficient, but not excessive, as the assays were optimized incrementally to reduce non-specificity.

A best-fit non-linear saturation curve for each mAb assay (mean of all peptide transitions) is provided in Figure 3 for [$bound_{cTn}$] versus [$free_{cTn}$]. The highest affinity binder (lowest K_d) among the mAbs was determined to be antibody 19C7, with a mean $K_d = 6.9 \times 10^{-8} \pm 3.3 \times 10^{-8}$ mol/L. Table 3a provides the dissociation constants of all other mAb-bead conjugates quantified in this manner. Mean K_d's range over two orders of magnitude from 6.9×10^{-8} mol/L (19C7) to 1.8×10^{-6} mol/L (M18) with a median $K_d = 1.2 \times 10^{-7}$ mol/L and a mean K_d among all mAbs = 4.2×10^{-7} mol/L mol/L. The antibody panel is separated statistically into three discrete groupings with mAbs 19C7, 560, MF4, and 267 being statistically indistinguishable as the optimal binders, and mAbs 3C7 and M18 being poorer choices, in that order. Table 3b details K_d constants determined for individual peptide transitions. Two optimal 'capture' mAbs as determined from this work (19C7 and 560) do support the results determined by the IFCC WG-TNI, and moreover, are known to bind the cTnI 'stable region', making them suitable choices for ELISA development. However, because the IFCC's evaluation of the optimal capture mAb was determined using a pair-wise assessment, we cannot directly compare the analytical approaches; instead we should view their results as supporting one another. Here, application of the ID LC-MS/MS approach is meant only to demonstrate its general use as a complementary quantitative tool along with immunoassays for the initial selection of antibodies for subsequent ELISA development.

The use of isotopically labeled peptides (as opposed to labeled proteins) as an internal standard in our ID MS experiments means that the cTn digestion efficiency is not accounted for by the peptide calibration curves. It is therefore evident that different

tryptic peptides within the cTn complex yield different saturation curves that cluster for precursor-to-product ion transitions originating from the same tryptic peptide. We can use corresponding transitions from a single tryptic peptide as validation of the ID MS measurements. Further, we can directly compare data from each peptide transition for all mAbs. Figure 4 demonstrates how peptide transitions will produce dissimilar saturation curves due to differences in digestion efficiencies, while transitions originating from the same tryptic peptides cluster together. Similarly, Table 4 provides a representative data set of K_d constants and R_T values determined for each transition of antibody 19C7 demonstrating the effect of digestion efficiencies. Dissimilar data observed between tryptic peptides suggests that we are making relative measurements and that saturation curves from these data sets represent relative K_d constants (non-intrinsic K_d) specific not only to the efficiency of the enzymatic digestion for a particular peptide, but also to the use of a solid support during the IP. The goal of the experiment is to quantitatively differentiate binding affinities of each mAb to cTnI under these given conditions. Therefore, the optimal 'capture' mAb can be determined by either comparing K_d constants from a single peptide transition across all mAb assays, or by comparing K_d constants using the mean of all peptide transition data for each antibody. In both cases, within error limits, the relative K_d among all mAbs is unchanged. Figure 5 shows a representative plot of the K_d constants determined for a) the individual transition 450.3 / 572.4, and b) for the mean of all transitions of all mAb assays (95% confidence interval). A similar pattern is observed for other individual peptide transitions as detailed in Table 3b. This data suggests that the top four performing mAbs in our panel are in fact, indistinguishable within error limits. This is not surprising noting that our mAb panel was pre-screened for the best available choices prior to this work. Nonetheless, the ID MS/MS approach is successful in further eliminating mAbs 3C7 and M18 from further consideration. Future work aims to express isotopically-labeled cTn complex in a native three-dimensional state to use as an internal standard to be spiked into the assay prior to enzymatic digestion, and which will account for variability in peptide digestion efficiency.

It is apparent that reproducibility of an immunoassay is highly dependant on the preparation of the mAb-magnetic bead conjugate. We tested reproducibility of our experimental technique for preparation of the mAb-bead conjugate by preparing three unique batches of mAb-bead conjugates for the antibody 19C7 and implementing equivalent immunoassays, tryptic digestions, and ID LC-MS/MS quantification. Independent curves were fit for each series of replicates. Significant differences between the replicates were tested at 95% confidence limits. In all cases, the K_d, and R_T constants were found to be indistinguishable for any given transition, and could therefore be treated as a single data set. Figure 6 illustrates 95% confidence intervals for data sets of each peptide transition. In Table 5 we provide values of the K_d parameter with error limits when estimated by a series of replicates for each transition. In this example, it is also demonstrated that data cluster among tryptic peptide precursor ions.

The incorporation of isotopically-labeled IgG peptides in our internal standard is useful for estimating the amount of mAb bound to the magnetic bead surface – regardless of orientation. All mAbs were assumed to be proportionally crosslinked to the bead surface

in all orientations so that the amount of 'active' Ab remained consistent between assays. Tryptic digestions of cTn (bound to mAb) were performed directly on the bead surfaces; therefore we are capable of measuring mAb tryptic peptides simultaneously with cTn peptides during LC-MS/MS analysis. Isotopically labeled IgG peptides for each mAb isotype were incorporated into the internal standards as discussed above. The concentration of IgG at all points on the saturation curve was quantified and used as a normalization factor for $cTnI_{free}$ to account for differences in the amount of mAb-bead added at any given cTn concentration. In most cases, this normalization factor approximates a value of one (see Supplementary Table 3), as any minor quantitative differences are attributed to pipetting inconsistencies or microheterogeneity of the slurry. The ability of MRM assays to simultaneously quantify many analytes allows us to use this mass spectrometry-based approach rather than relying on accurate calibration of a pipette, or on gravimetry which assumes increasing error at very low volumes.

The results discussed here for the selection of an optimal 'capture' mAb were found to be in agreement with those determined by the IFCC WG-TNI using orthogonal approaches [10]. Quantitative accuracy and precision of ID MS techniques, and the selectivity and specificity of MRM measurements can provide necessary confidence to ELISA antibody selections [18]. Although it is not a high-throughput approach, ID LC-MS/MS possesses superior robustness and reproducibility compared to ELISA; this platform can monitor hundreds of measurands simultaneously within an assay, and can validate quantitative results concurrently using multiple signature peptides and multiple transitions per peptide. Here we demonstrate that MS-based selection of antibodies is an ideal complementary tool to immunoassay development.

Future work and conclusions

We have shown that an LC-MS/MS immunoassay platform can quantitatively select optimal mAbs to be used as 'capture' antibodies for development of an ELISA. Based on data of relative K_d constants, we have selected clone 19C7 as a candidate 'capture' mAb for further development. Next, we will use the mAb 19C7 (still crosslinked to a magnetic bead support) in a pair-wise analysis with each of the five other mAbs in our pre-screened panel employed as free antibodies in solution but tagged with an alkaline phosphatase label. An LC-MS/MS quantitative immunoassay similar to that shown here will be used to rank the binding affinity of the five 'detection' mAbs individually, and also within a competitive immunoassay. A well-characterized secondary reference procedure based on ELISA measurements will provide the clinical community the necessary tools for inter- and intra-laboratory standardization of troponin I quantification with essential metrological traceability. Mass spectrometry is shown to be an invaluable complementary tool for immunoassay development and antibody characterization.

Acknowledgements

The authors would like to thank Eric Kilpatrick of the Analytical Chemistry Division at NIST (Charleston, SC) for his work in characterizing IgG tryptic peptides using LC-MS/MS (MRM) selection assays.

Reference List

1. **Katus HA, Remppis A, Neumann FJ, Scheffold T, Diederich KW, Vinar G, Noe A, Matern G, and Kuebler W (1991) Circulation 83:902-912.**

2. **Bodor GS, Porter S, Landt Y, and Ladenson JH (1992) Clinical Chemistry 38:2203-2214.**

3. **Wu AHB, Valdes R, Apple FS, Gornet T, Stone MA, Mayfieldstokes S, Ingersollstroubos AM, and Wiler B (1994) Clinical Chemistry 40:900-907.**

4. **Larue C, Calzolari C, Bertinchant JP, Leclercq F, Grolleau R, and Pau B (1993) Clinical Chemistry 39:972-979.**

5. **Wu AHB, Feng YJ, Moore R, Apple FS, McPherson PH, Buechler KF, and Bodor G (1998) Clinical Chemistry 44:1198-1208.**

6. **Zethelius B, Johnston N, and Venge P (2006) Circulation 113:1071-1078.**

7. **Christenson RH, Duh SH, Apple FS, Bodor GS, Bunk DM, Panteghini M, Welch MJ, Wu AHB, and Kahn SE (2006) Clinical Chemistry 52:1685-1692.**

8. **Christenson RH, Duh S, Apple FS, Bodor G, Panteghini M, Welch M, Wu AH, and Kahn SE (2006) Clinical Chemistry 52:D6.**

9. **Katrukha AG, Bereznikova AV, Filatov VL, Esakova TV, Kolosova OV, Pettersson K, Lovgren T, Bulargina TV, Trifonov IR, Gratsiansky NA, Pulkki K, Voipio-Pulkki LM, and Gusev NB (1998) Clinical Chemistry 44:2433-2440.**

10. **Noble, Bunk, He, and Wang. Development of a Candidate Secondary Reference Procedure (Immunoassay Based Measurement Procedure of Higher Metrological Order) for Cardiac Troponin I: I. Antibody Characterization and Preliminary Validation. Clinical Chemisty and Laboratory Medicine . 2010.**

Ref Type: In Press

11. **Katrukha AG, Bereznikova AV, Esakova TV, Pettersson K, Lovgren T, and Severina ME (1997) Clinical Chemistry 43:1379-1385.**

12. **Certificate of Analysis, Standard Reference Material,¥ 2921, Human Cardiac Troponin Complex. 1-28-0010.**

Ref Type: Online Source

13. **Liao WL, Heo GY, Dodder NG, Pikuleva IA, and Turko IV (2010) Analytical Chemistry 82:5760-5767.**

14. http://orgmassspecr.r-forge.r-project.org/. [OrgMassSpecR computer program]. 2010.
Ref Type: Computer Program

15. Kutner M, Nachtsheim CJ, Neter J, and Li W (2005) Applied Linear Statistical Models. McGraw Hill.

16. Bates D.M and Watts D.G. (1988) Nonlinear regression analysis and its applications. Wiley.

17. R Development Core Team. R: A Language and Environment for Statistical Computing. http://www.R-project.org . 2010.
Ref Type: Electronic Citation

18. Ackermann BL and Berna MJ (2007) Expert Review of Proteomics 4:175-186.

19. Solaro RJ and van der Velden J (2010) Journal of Molecular and Cellular Cardiology 48:810-816.

20. Metzger JM and Westfall MV (2004) Circulation Research 94:146-158.

21. Kobayashi T and Solaro RJ (2005) Annual Review of Physiology 67:39-67.

22. Solaro RJ, Moir AJG, and Perry SV (1976) Nature 262:615-617.

23. Moir AJG, Solaro RJ, and Perry SV (1980) Biochemical Journal 185:505-513.

24. (1989) Antigen-Antibody Interactions and Monoclonal Antibodies. In: Fundamental Immunology. Raven Press Ltd, New York, NY.

25. Schiel JE, Mallik R, Soman S, Joseph KS, and Hage DS (2006) Journal of Separation Science 29:719-737.

26. (2005) Immobilization Methods for Affinity Chromatography, Immunoaffinity Chromatography. In: Handbook of Affinity Chromatgraphy. CRC Press.

27. Vuignier K, Schappler J, Veuthey JL, Carrupt PA, and Martel S (2010) Analytical and Bioanalytical Chemistry 398:53-66.

Table 1

AA Sequence	Isotopic label	cTn subunit / IgG isotype	Theoretical MW (g/mol)		Retention time (min)
			Unlabeled	Labeled	
NITEIAD**L*** TQK	$^{13}C6$	cTnI	1246.4	1252.4	19.5
TLLLQ**I*** AK	$^{13}C6$	cTnI	900.2	906.2	21.2
NIDA**L*** SGMEGR	$^{13}C6$	cTnI	1163.3	1169.3	18.0
VLAIDHLNEDQ**L*** R	$^{13}C6$	cTnT	1536.7	1542.7	18.7
AAVEQ**L*** TEEQK	$^{13}C6$	cTnC	1246.4	1252.4	14.2
VNSAAFPAP**I*** EK	$^{13}C6$, ^{15}N	IgG1	1244.7	1251.1	17.9
NTEPVLDSDGSY**F*** MYSK	$^{13}C9$, ^{15}N	IgG2a	1954.9	1963.4	21.2
DLPSP**I*** ER	$^{13}C6$, ^{15}N	IgG2b	926.8	933.2	17.0

bold* = site of isotopic label

Table 2

Peptide	Transition	Precursor/ product ion charge state	Fragment ion	DP	EP	CE	CXP
NITEIADLTQK	623.3 → 675.4	+2 / +1	y6	65	9	27	22
	623.3 → 1018.5	+2 / +1	y9	65	10	27	22
NITEIAD**L*** TQK	626.3 → 681.4	+2 / +1	y6	65	9	27	22
	626.3 → 1024.5	+2 / +1	y9	65	10	27	22
TLLLQIAK	450.3 → 572.4	+2 / +1	y5	54	10	22	23
	450.3 → 685.5	+2 / +1	y6	50	9	20	22
TLLLQ**I*** AK	453.3 → 578.4	+2 / +1	y5	54	10	22	23
	453.3 → 691.5	+2 / +1	y6	50	9	20	22
NIDALSGMEGR	581.8 → 749.4	+2 / +1	y7	54	9	27	22
	581.8 → 935.4	+2 / +1	y9	55	9	26	27
NIDA**L*** SGMEGR	584.8 → 755.4	+2 / +1	y7	54	9	27	22
	584.8 → 941.4	+2 / +1	y9	55	9	26	27
VLAIDHLNEDQLR	512.6 → 662.3	+3 / +2	y11	52	8.5	20.5	21.5
	512.6 → 718.9	+3 / +2	y12	52	8.5	22	23
VLAIDHLNEDQ**L*** R	514.6 → 685.3	+3 / +2	y11	52	8.5	20.5	21.5
	514.6 → 721.9	+3 / +2	y12	52	8.5	22	23
AAVEQLTEEQK	623.3 → 747.4	+2 / +1	y6	65	8.5	30.25	26
	623.3 → 1004.5	+2 / +1	y8	66	8.5	29.35	27.5
AAVEQ**L*** TEEQK	626.3 → 753.4	+2 / +1	y6	65	8.5	30.25	26
	626.3 → 1010.5	+2 / +1	y8	66	8.5	29.35	27.5
VNSAAFPAPIEK	622.3 → 654.4	+2 / +1	y6	57	9	27.5	22.35
	622.3 → 801.5	+2 / +1	y7	57.7	9	25.4	26
VNSAAFPAP**I*** EK	625.8 → 661.4	+2 / +1	y6	57	9	27.5	22.35
	625.8 → 808.5	+2 / +1	y7	57.7	9	25.4	26
NTEPVLDSDGSYFMYSK	651.6 → 675.3	+3 / +1	y5	50	8.5	21	24
	651.6 → 838.4	+3 / +1	y6	51	8.5	21.8	29.5
NTEPVLDSDGSY**F*** MYSK	655.0 → 685.3	+3 / +1	y5	50	8.5	21	24
	655.0 → 848.4	+3 / +1	y6	51	8.5	21.8	29.5
DLPSPIER	463.8 → 514.3	+2 / +1	y4	41.7	9	27.4	17.1
	463.8 → 698.4	+2 / +1	y6	40	9	18.6	22.5
DLPSP**I*** ER	467.3 → 521.3	+2 / +1	y4	41.7	9	27.4	17.1
	467.3 → 705.4	+2 / +1	y6	40	9	18.6	22.5

*DP = declustering potential
*EP = entrance potential
*CE = collision energy
*CXP = cell exit potential

Table 3

a) Mean K_d for α-cTnI mAbs (all peptide transitions)

Antibody	mean K_d, µmol/L	standard deviation, µmol/L
19C7	0.0687	0.033
560	0.108	0.078
MF4	0.112	0.061
267	0.117	0.078
3C7	0.400	0.091
M18	1.75	0.86

b) K_d determined for all mAb assays, individual peptide transitions

	transition									
Antibody	**450.3 / 572.4**	**450.3 / 685.5**	**623.3 / 1018.5**	**623.3 / 675.4**	**581.8 / 749.4**	**581.8 / 935.4**	**623.3 / 1004.5**	**623.3 / 747.4**	**512.6 / 662.3**	**512.6 / 718.9**
19C7	0.0200	0.0301	0.0563	0.0342	0.0892	0.0796	0.109	0.117	0.0807	0.0700
560	0.0264	0.0433	0.0800	0.0461	0.103	0.0967	0.174	0.294	0.113	0.105
267	0.0174	0.0330	0.0710	0.0371	0.148	0.138	0.257	0.208	0.132	0.130
MF4	0.0252	0.0435	0.0847	0.0463	0.163	0.155	0.178	0.197	0.121	0.109
3C7	0.318	0.299	0.337	0.321	0.465	0.537			0.449	0.477
M18	1.08	0.787	1.95	3.17	1.01	1.75			2.79	1.45

Table 4

K_d and R_T for related transitions from tryptic peptides cluster similarly

Peptide	Transition	K_d	R_T
AAVEQLTEEQK	623.3 → 1004.5	0.116	0.0131
AAVEQLTEEQK	623.3 → 747.4	0.125	0.0103
NIDALSGMEGR	581.8 → 749.4	0.0975	0.0300
NIDALSGMEGR	581.8 → 935.4	0.0875	0.0238
VLAIDHLNEDQLR	512.6 → 662.3	0.0867	0.0270
VLAIDHLNEDQLR	512.6 → 718.9	0.0770	0.0337
NITEIADLTQK	623.3 → 1018.5	0.0585	0.0514
NITEIADLTQK	623.3 → 675.4	0.0363	0.0758
TLLQIAK	450.3 → 572.4	0.0226	0.100
TLLQIAK	450.3 → 685.5	0.0322	0.0815

Table 5

K_d and expanded uncertainty for triplicate bead preparations of mAb 19C7

Peptide	Transition	K_d	Expanded uncertainty
AAVEQLTEEQK	623.3 → 1004.5	0.0732	0.0303
AAVEQLTEEQK	623.3 → 747.4	0.124	0.0404
NIDALSGMEGR	581.8 → 749.4	0.102	0.0437
NIDALSGMEGR	581.8 → 935.4	0.105	0.0338
NITEIADLTQK	623.3 → 1018.5	0.0744	0.0174
NITEIADLTQK	623.3 → 675.4	0.0787	0.0274
TLLQIAK	450.3 → 572.4	0.0275	0.0168
TLLQIAK	450.3 → 685.5	0.0343	0.0129

Figure 1 – human cardiac troponin I
(amino acid sequence, mAb binding epitopes)

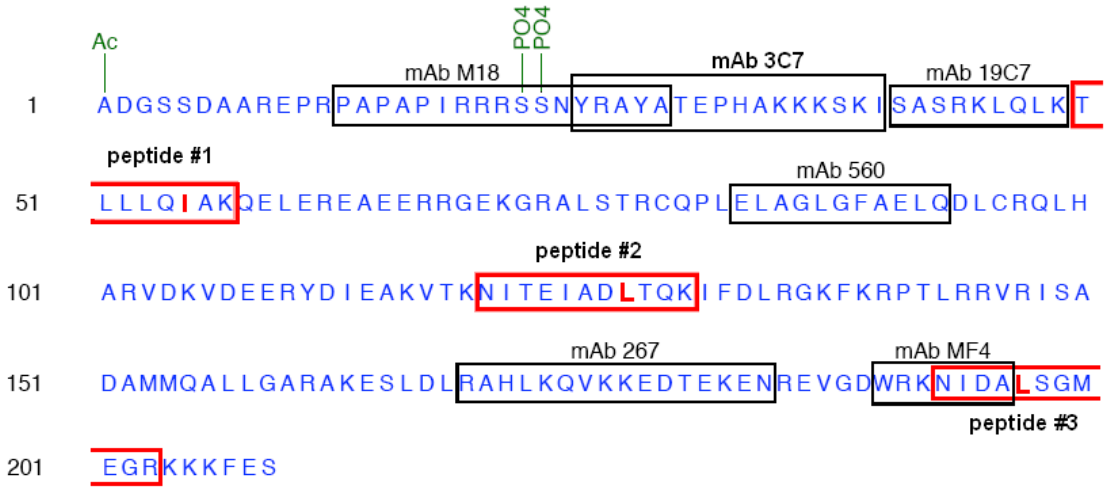

Figure 2 – representative MRM TIC for cTn digest (IgG_{2b} mAb)

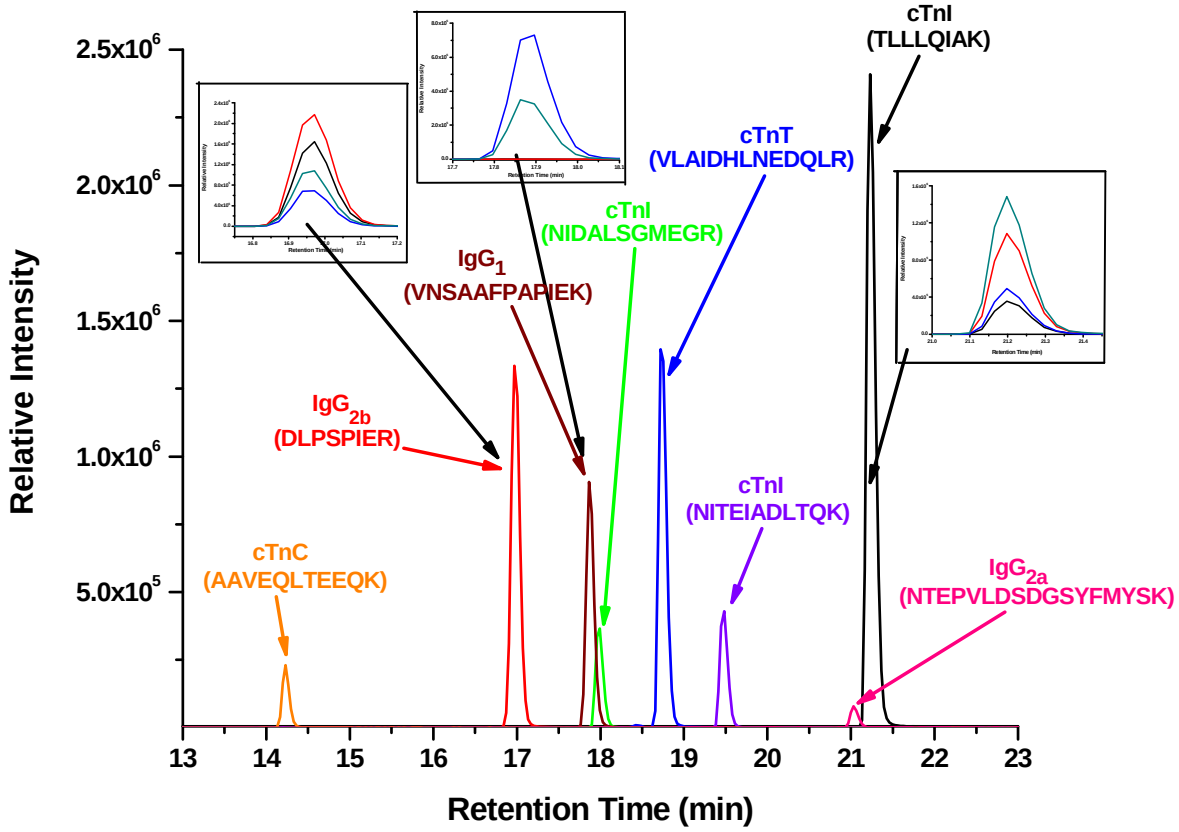

Figure 3 – Mean K_d curves with 95% confidence intervals for all mAbs

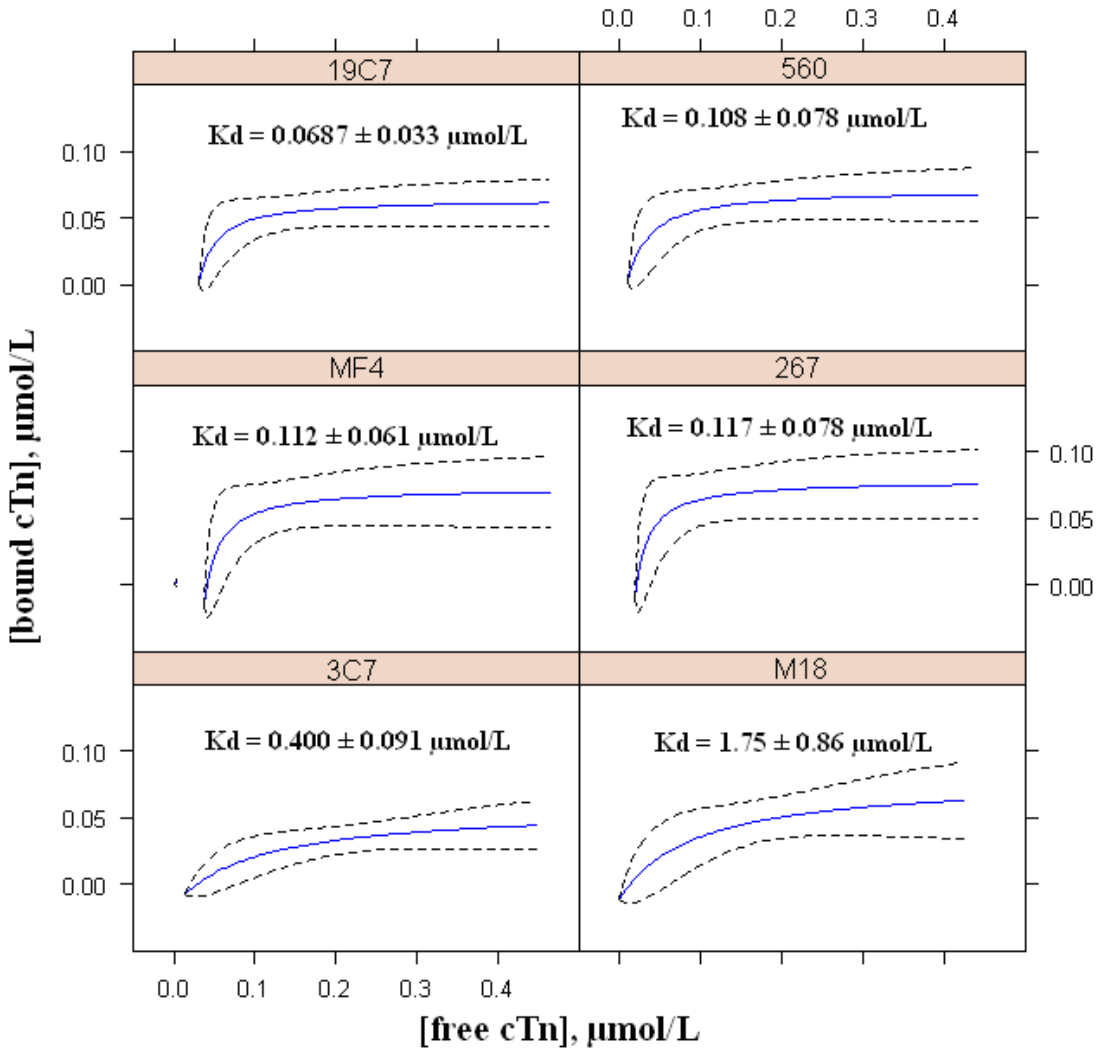

Figure 4 – Peptide transitions produce dissimilar saturation curves due to digestion efficiency variations

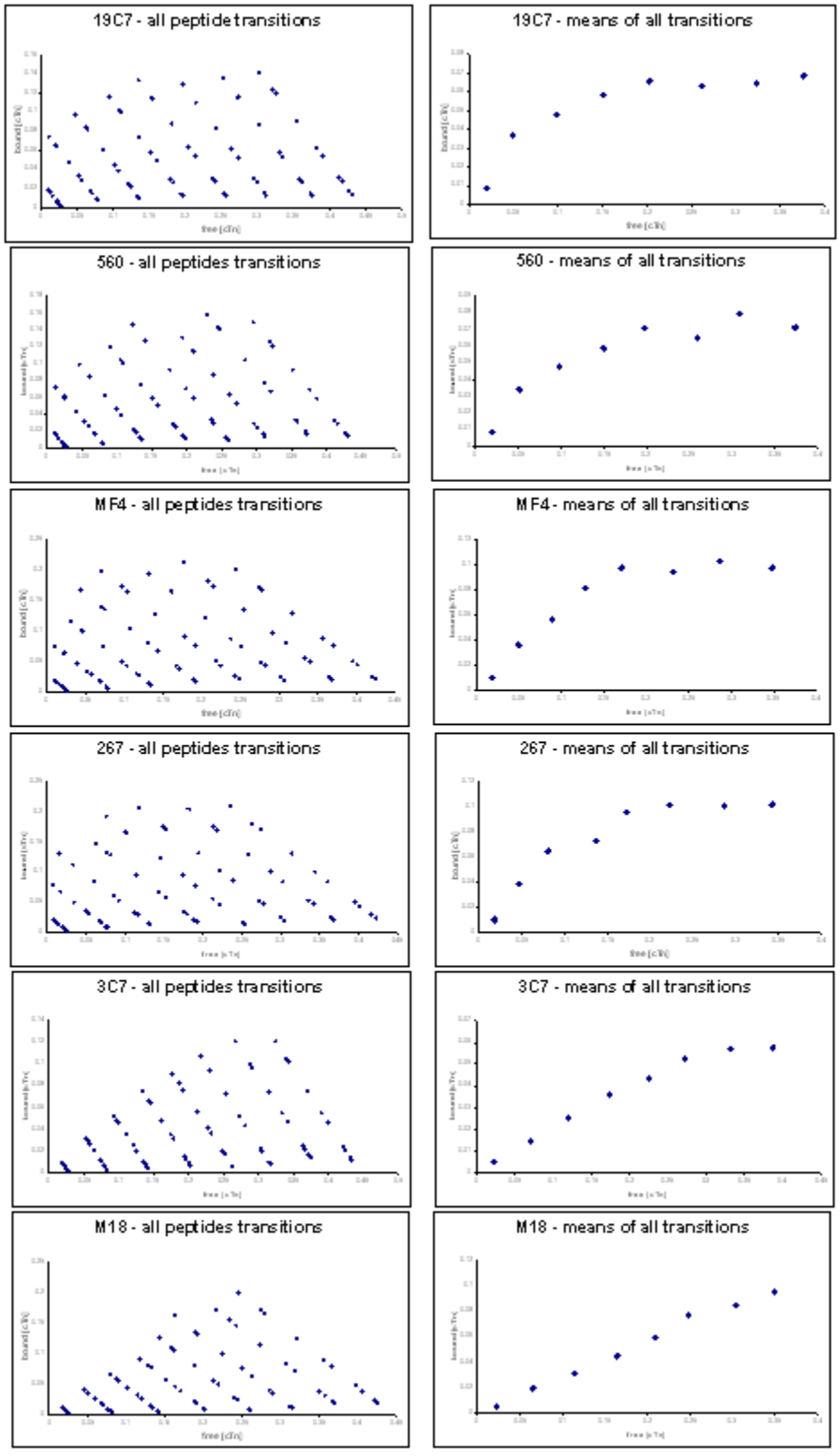

Figure 5

a)

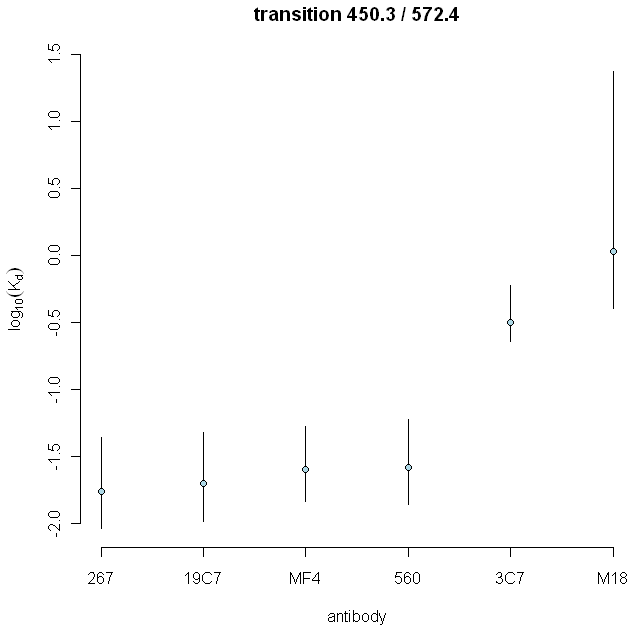

b)

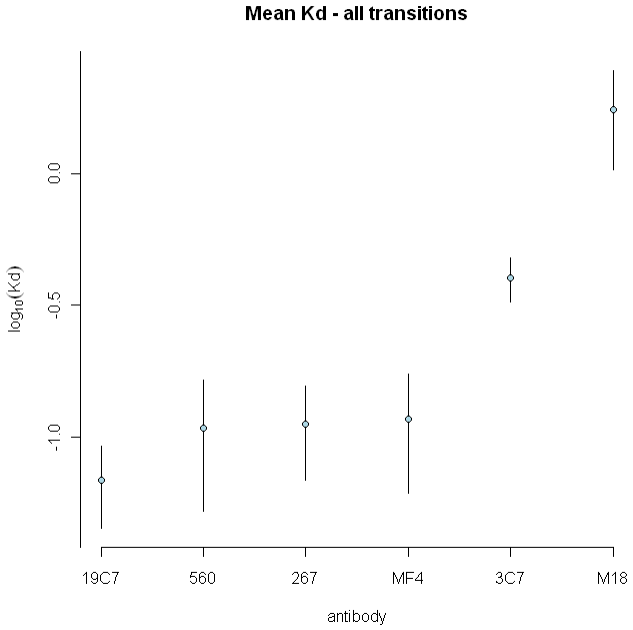

These plots show a) K_d estimates for each mAb considering representative peptide transition 450.3 / 572.4, and b) the mean of the K_d estimates considering all peptide transitions for each antibody with all error bars indicating a 95% confidence interval of the mean

Figure 6 – K_d curves for each peptide transition, mAb 19C7, triplicate preparation

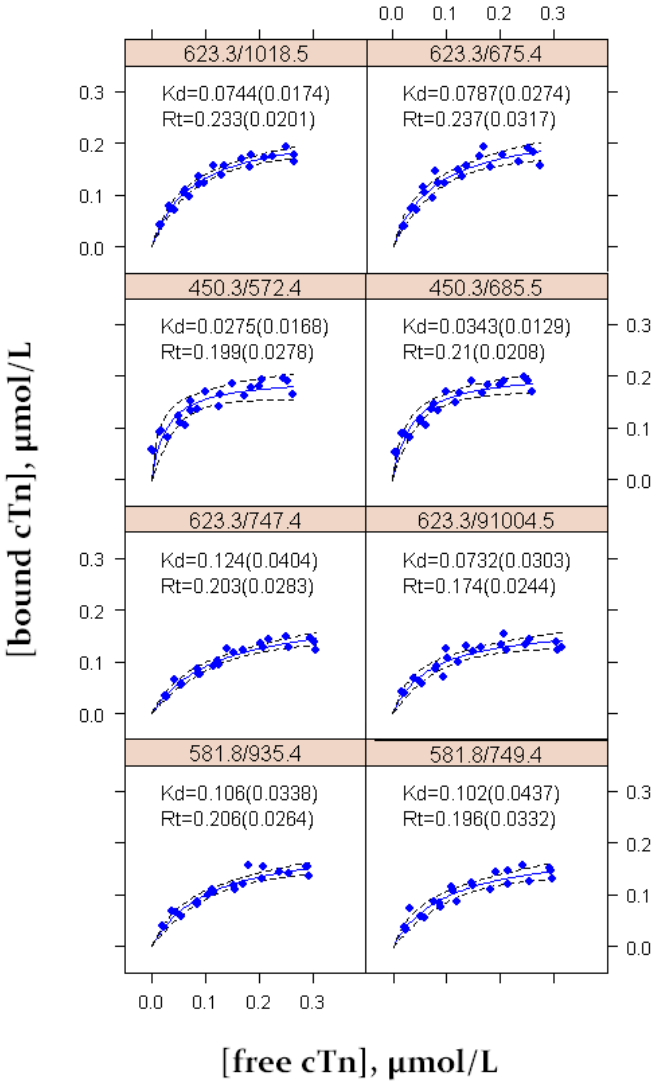

Supplementary Data

R code for obtaining the confidence band of the mean response

```
# data structure of cTn.data is
# data.frame(antibody, sample, transition, bound.cTn, free.cTn)
…
require(lattice)
require(MASS)
tran.lev<- levels(as.factor(cTn.data$transition))
X11()
print(xyplot(bound.cTn ~ free.cTn | transition,
    data = cTn.data,
    xlab = "[free cTn], uM",
    ylab = "[bound cTn], uM",
    xlim = c(-0.05, 0.4),
    ylim = c(-0.05, 0.35),
    col = "blue",
    pch = 19,
    layout = c(3, 3),
    main = paste("Antibody 19C7", " samples a to h", sep = ""),
    panel = function(x, y, groups, subscripts, ...) {
      res.nls <- nls(y ~ (Rt * x) / (Kd + x), start = list(Rt = max(y), Kd = max(min(x),
x[y>max(y)/2][1])))
       theta<- coefficients(res.nls)
       # plot the predicted value
      panel.curve((theta[1] * x) / (theta[2] + x), from = 0, to = max(x), col = "blue")
       # obtain the confidence band
       theta.se<- summary(res.nls)$parameters[,2]
       pred<- predict(res.nls)
       n<- length(pred)
       p<- length(theta)
       sigma<- summary(res.nls)$sigma
       V<- attributes(res.nls$m$resid())$gradient
       qr.res<- qr(V)
       R1<- qr.R(qr.res)
       x.0<- c(0:100)/100*max(x)
       v.0<- cbind(x.0/(theta[2]+x.0), -(theta[1])*x.0/(theta[2]+x.0)^2)
       R1.inv<- ginv(R1)
       r.0<- v.0 %*% R1.inv
       d.0<- r.0[,1]
       for (k in 1:101) d.0[k]<- sqrt(sum(r.0[k,]^2))
       panel.curve(theta[1]*x/(theta[2]+x)+sigma*d.0*sqrt(p*qf(0.975,p,n-p)), from=0.0,
to=max(x), n=101, col=1, lty=2, add=T)
       panel.curve(theta[1]*x/(theta[2]+x)-sigma*d.0*sqrt(p*qf(0.975,p,n-p)), from=0.0,
to=max(x), n=101, col=1, lty=2, add=T)

      panel.xyplot(x, y, ...)
      panel.text(0, 0.3, labels = paste("Kd=", signif(theta[2], 3),"(",signif(qt(0.975,n-
p)*theta.se[2],3),")", sep = ""), pos = 4, cex = 0.9)
      panel.text(0, 0.25, labels = paste("Rt=", signif(theta[1],
3),"(",signif(qt(0.975,n-p)*theta.se[1],3),")", sep = ""), pos = 4, cex = 0.9)
    }
  ))
```

Supplementary Figure 1 – IgG peptides, MRM screening
(NCBI protein database – constant region only based on alignment of multiple sequences)

a) IgG_1

>gi|148540420|gb|ABQ85914.1| immunoglobulin gamma 1 heavy chain precursor [Mus musculus]

AKTTPPSVYPLAPGSAAQTNSMVTLGCLVKGYFPEPVTVTWNSGSLSSGVHTFPAVLQSDLYTLSSSVTVPSST
WPSETVTCNVAHPASSTKVDKKIVPRDCGCKPCICTVPEVSSVFIFPPKPK**DVLTITLTPK**VTCVVVDISKDDP
EVQFSWFVDDVEVHTAQTQPREEQFNSTFR**SVSELPIMHQDWLNGK**EFKCR**VNSAAFPAPIEK**TISKTKGRP
K**APQVYTIPPPK**EQMAKDKVSLTCMITDFFPEDITVEWQWNGQPAENYK**NTQPIMDTDGSYFVYSK**LNVQ
KSNWEAGNTFTCSVLHEGLHNHHTEKSLSHSPGK

TIC of MRM analysis of IgG_1 mAb digest

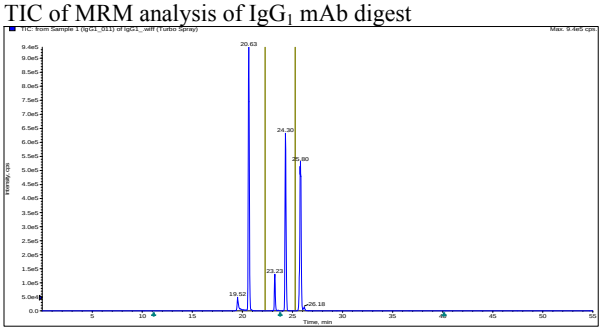

MALDI analysis of IgG_1 mAb digest

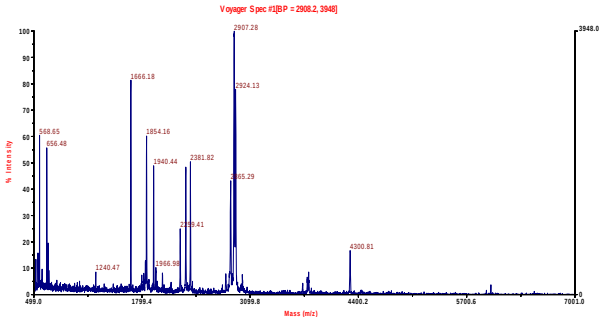

b) IgG_{2a}

>gi|194438|gb|AAB59660.1| immunoglobulin gamma 2A chain [Mus musculus]

KTTAPSVYPLAPVCGDTTGSSVTLGCLVKGYFPEPVTLTWNSGSLSSGVHTFPAVLQSDLYTLSSSVTVT
SSTWPSQSITCNVAHPASSTKVDKKIEPRGPTIKPCPPCKCPAPNLLGGPSVFIFPPKIKDVLMISLSPI
VTCVVVDVSEDDPDVQISWFVNNVEVHTAQTQTHREDYNSTLR**VVSALPIQHQDWMSGK**EFKCKVNNKDL
PAPIERTISKPKGSVR**APQVYVLPPPEEEMTK**KQVTLTCMVTDFMPEDIYVEWTNNGKTELNYK**NTEPVL**
DSDGSYFMYSKLRVEKKNWVERNSYSCSVVHEGLHNHHTTKSFSRTPGK

TIC of MRM analysis of IgG_{2a} mAb digest

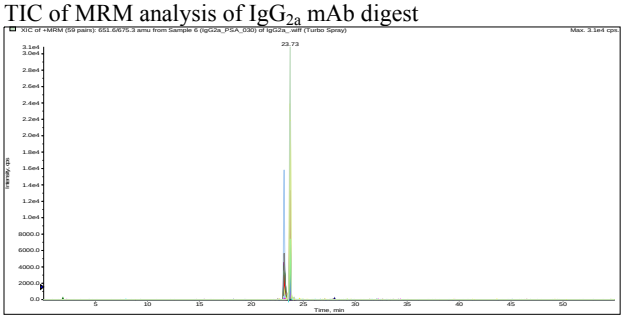

MALDI analysis of IgG_{2a} mAb digest

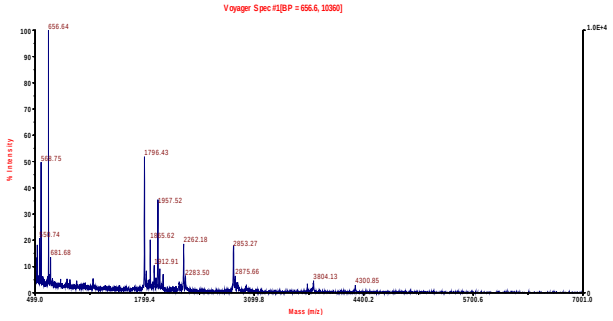

b) IgG_{2b}

>gi|54827|emb|CAA47649.1| immunoglobulin gamma 2b heavy chain [Mus musculus]

ALLQSGLYTMSSSVTVPSSTWPSQTVTCSVAHPASSTTVDKKLEPSGPISTINPCPPCKECHKCPAPNLEGGPSV
FIFPPNIKDVLMISLTPKVTCVVVDVSEDDPDVQISWFVNNVEVHTAQTQTHREDYNSTIR**VVSTLPIQHQDW**
MSGKEFKCKVNNK**DLPSPIER**TISKIKGLVR**APQVYILPPPAEQLSRK**DVSLTCLVVGFNPGDISVEWTSNGH
TEENYKDTAPVLDSDGSYFIYSKLNMKTSKWEKTDSFSCNVRHEGLKNYYLKKTISRSPGK

TIC of MRM analysis of IgG_{2b} mAb digest

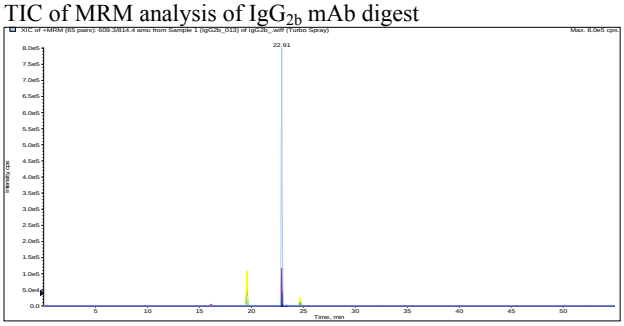

MALDI analysis of IgG_{2b} mAb digest

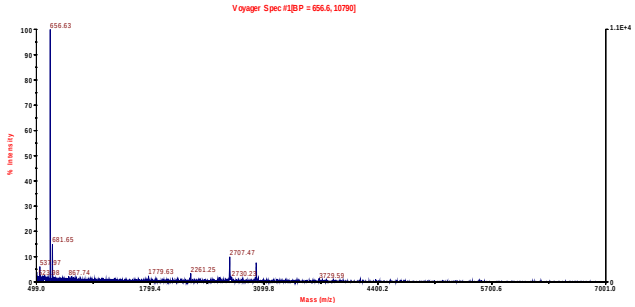

Supplementary Figure 2 – Calibration curves of cTn peptide transitions

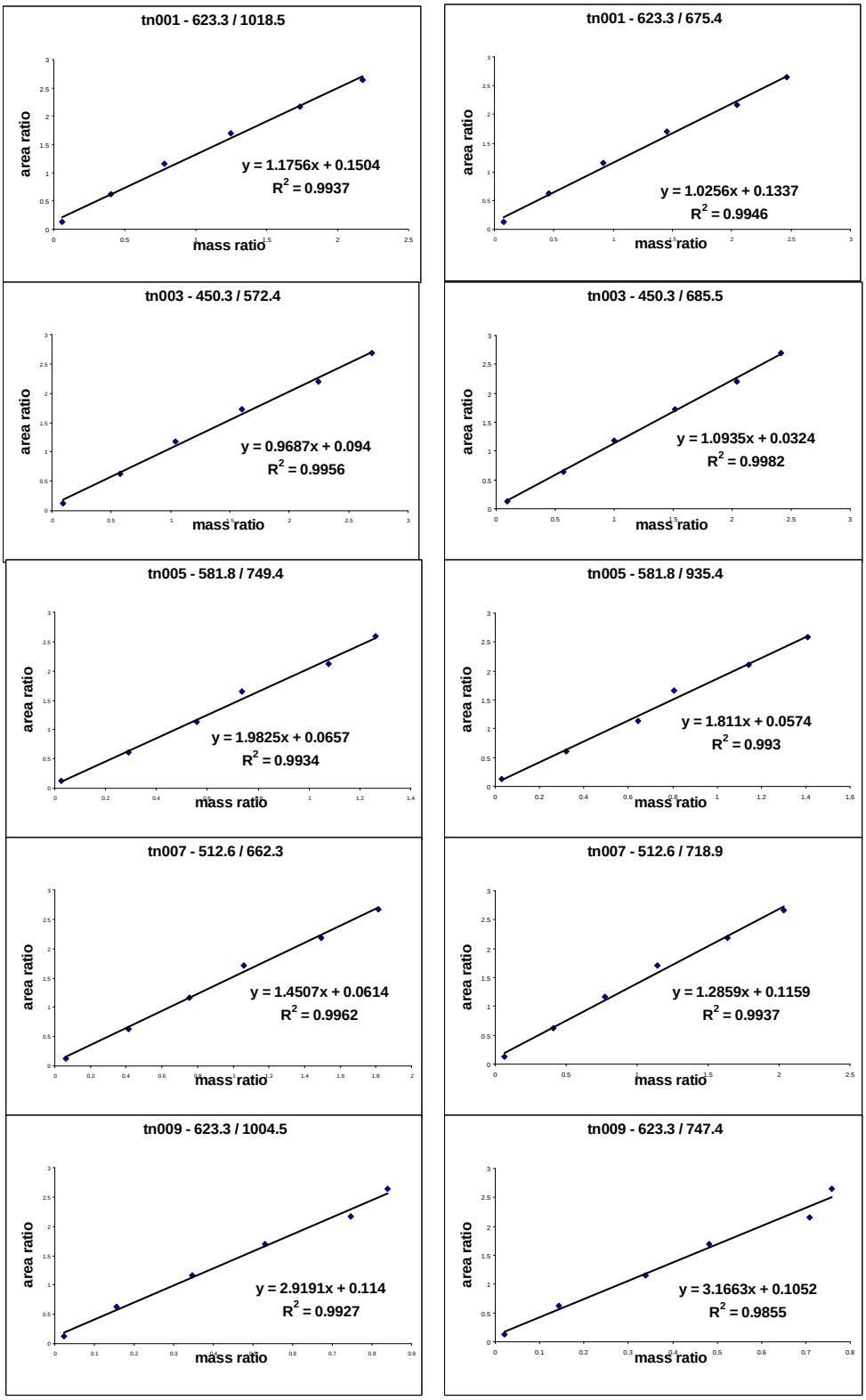

Supplementary Table 1

	cTn peptide molar mass ratio (unlabeled / labeled)				
sample	**NITEIADLTQK**	**TLLLQIAK**	**NIDALSGMEGR**	**VLAIDHLNEDQLR**	**AAVEQLTEEQK**
A	0.1548	0.1574	0.1513	0.1562	0.1546
B	0.4696	0.4775	0.4589	0.4737	0.4690
C	0.8050	0.8186	0.7866	0.8120	0.8040
D	1.1575	1.1771	1.1311	1.1676	1.1561
E	1.4840	1.5091	1.4502	1.4969	1.4822
F	1.7965	1.8268	1.7555	1.8121	1.7943
G	2.1480	2.1842	2.0989	2.1666	2.1453
H	2.4604	2.5019	2.4042	2.4818	2.4574
calibrant 1	0.1231	0.1251	0.1203	0.1241	0.1229
calibrant 2	0.6239	0.6344	0.6096	0.6293	0.6231
calibrant 3	1.1575	1.1771	1.1311	1.1676	1.1561
calibrant 4	1.6949	1.7235	1.6563	1.7097	1.6929
calibrant 5	2.1636	2.2001	2.1142	2.1824	2.1609
calibrant 6	2.6479	2.6925	2.5874	2.6708	2.6446

Supplementary Table 2

mAb isotype	Candidate peptide sequence	Retention time (minutes)	Molecular mass (g/mol)
IgG_1	APQVYTIPPPK	19.5	1210.7
IgG_1	VNSAAFPAPIEK*	20.6	1243.7
IgG_1	NTQPIMDTDGSYFVYSK	23.2	1965.9
IgG_1	DVLTITLTPK	24.3	1100.7
IgG_1	SVSELPIMHQDWLNGK	25.8	1853.9
IgG_{2a}	VVSALPIQHQDWMSGK	23.1	1795.9
IgG_{2a}	APQVYVLPPPEEEMTK	23.1	1827.9
IgG_{2a}	NTEPVLDSDGSYFMYSK*	23.8	1952.9
IgG_{2b}	DLPSPIER*	19.6	926.5
IgG_{2b}	VVSTLPIQHQDWMSGK	22.9	1825.9
IgG_{2b}	APQVYILPPPAEQLSR	24.7	1779.0

* = peptides synthesized as isotopically-labeled internal standard

Supplementary Table 3

Sample	IgG transition	[IgG], µmol/L	normalized [IgG], µmol/L	normalization factor
19C7-a	IgG2b - 463.8 / 514.3	0.811787078	0.962973995	0.956
19C7-a	IgG2b - 463.8 / 698.4	0.726800822	0.948826138	
19C7-b	IgG2b - 463.8 / 514.3	0.84283193	0.999800629	1.000
19C7-b	IgG2b - 463.8 / 698.4	0.765841641	0.999793265	
19C7-c	IgG2b - 463.8 / 514.3	0.797348063	0.945845864	0.933
19C7-c	IgG2b - 463.8 / 698.4	0.704402988	0.919586147	
19C7-d	IgG2b - 463.8 / 514.3	0.784289232	0.930354961	0.926
19C7-d	IgG2b - 463.8 / 698.4	0.705505332	0.921025237	
19C7-e	IgG2b - 463.8 / 514.3	0.843065448	1.000077636	0.992
19C7-e	IgG2b - 463.8 / 698.4	0.753523992	0.983712784	
19C7-f	IgG2b - 463.8 / 514.3	0.812406682	0.963708995	0.967
19C7-f	IgG2b - 463.8 / 698.4	0.743802097	0.971021014	
19C7-g	IgG2b - 463.8 / 514.3	0.821023608	0.973930733	0.980
19C7-g	IgG2b - 463.8 / 698.4	0.755334807	0.986076771	
19C7-h	IgG2b - 463.8 / 514.3	0.842086045	0.99891583	0.994
19C7-h	IgG2b - 463.8 / 698.4	0.756981683	0.98822674	
267-a	IgG2a - 651.6 / 675.3	0.578604505	0.895672608	0.851
267-a	IgG2a - 651.6 / 838.4	0.508044236	0.806419423	
267-b	IgG2a - 651.6 / 675.3	0.486640909	0.7533141	0.744
267-b	IgG2a - 651.6 / 838.4	0.462343997	0.73387936	
267-c	IgG2a - 651.6 / 675.3	0.521596241	0.807424522	0.802
267-c	IgG2a - 651.6 / 838.4	0.502437686	0.797520136	
267-d	IgG2a - 651.6 / 675.3	0.440183373	0.681398411	0.662
267-d	IgG2a - 651.6 / 838.4	0.404333633	0.641799418	
267-e	IgG2a - 651.6 / 675.3	0.645769029	0.99964246	1.000
267-e	IgG2a - 651.6 / 838.4	0.629870711	0.999794779	
267-f	IgG2a - 651.6 / 675.3	0.550401959	0.852015416	0.855
267-f	IgG2a - 651.6 / 838.4	0.540324958	0.857658664	
267-g	IgG2a - 651.6 / 675.3	0.534715118	0.827732381	0.794
267-g	IgG2a - 651.6 / 838.4	0.479412884	0.760972832	
267-h	IgG2a - 651.6 / 675.3	0.451972538	0.699647891	0.697
267-h	IgG2a - 651.6 / 838.4	0.437374627	0.694245439	
3C7-a	IgG1 - 622.3 / 654.4	0.661847216	0.938790377	0.951
3C7-a	IgG1 - 622.3 / 801.5	0.765493283	0.962884633	
3C7-b	IgG1 - 622.3 / 654.4	0.685178223	0.971884004	0.971
3C7-b	IgG1 - 622.3 / 801.5	0.771484256	0.970420448	
3C7-c	IgG1 - 622.3 / 654.4	0.660953864	0.937523211	0.950
3C7-c	IgG1 - 622.3 / 801.5	0.764815863	0.962032533	
3C7-d	IgG1 - 622.3 / 654.4	0.667256434	0.946463026	0.953
3C7-d	IgG1 - 622.3 / 801.5	0.762288372	0.958853298	
3C7-e	IgG1 - 622.3 / 654.4	0.666467017	0.945343286	0.954
3C7-e	IgG1 - 622.3 / 801.5	0.765688159	0.963129759	
3C7-f	IgG1 - 622.3 / 654.4	0.696708679	0.988239261	0.994
3C7-f	IgG1 - 622.3 / 801.5	0.794535892	0.999416216	
3C7-g	IgG1 - 622.3 / 654.4	0.70513989	1.000198425	0.999

3C7-g	IgG1 - 622.3 / 801.5	0.793963863	0.998696683	
3C7-h	IgG1 - 622.3 / 654.4	0.674218305	0.956338021	0.971
3C7-h	IgG1 - 622.3 / 801.5	0.783357576	0.985355442	
560-a	IgG1 - 622.3 / 654.4	0.458853865	0.942837406	0.971
560-a	IgG1 - 622.3 / 801.5	0.541229842	1.000000000	
560-b	IgG1 - 622.3 / 654.4	0.486673378	1.000000000	0.997
560-b	IgG1 - 622.3 / 801.5	0.538446162	0.994856751	
560-c	IgG1 - 622.3 / 654.4	0.437306237	0.898562067	0.909
560-c	IgG1 - 622.3 / 801.5	0.49816269	0.92042724	
560-d	IgG1 - 622.3 / 654.4	0.444639486	0.913630179	0.937
560-d	IgG1 - 622.3 / 801.5	0.520010355	0.960793945	
560-e	IgG1 - 622.3 / 654.4	0.435735928	0.895335451	0.891
560-e	IgG1 - 622.3 / 801.5	0.479632499	0.886190047	
560-f	IgG1 - 622.3 / 654.4	0.410453978	0.843386953	0.849
560-f	IgG1 - 622.3 / 801.5	0.462938627	0.855345716	
560-g	IgG1 - 622.3 / 654.4	0.452541993	0.929867984	0.935
560-g	IgG1 - 622.3 / 801.5	0.509017812	0.940483641	
560-h	IgG1 - 622.3 / 654.4	0.441481572	0.907141405	0.910
560-h	IgG1 - 622.3 / 801.5	0.494248066	0.913194411	
M18-a	IgG1 - 622.3 / 654.4	0.696158451	1.000000000	1.000
M18-a	IgG1 - 622.3 / 801.5	0.816665741	1.000000000	
M18-b	IgG1 - 622.3 / 654.4	0.681272594	0.978617143	0.987
M18-b	IgG1 - 622.3 / 801.5	0.813089807	0.995621301	
M18-c	IgG1 - 622.3 / 654.4	0.679400708	0.975928263	0.965
M18-c	IgG1 - 622.3 / 801.5	0.779429716	0.954404816	
M18-d	IgG1 - 622.3 / 654.4	0.666031495	0.956723996	0.952
M18-d	IgG1 - 622.3 / 801.5	0.773499267	0.947143034	
M18-e	IgG1 - 622.3 / 654.4	0.640651471	0.920266745	0.906
M18-e	IgG1 - 622.3 / 801.5	0.729045012	0.89270919	
M18-f	IgG1 - 622.3 / 654.4	0.678289133	0.974331537	0.974
M18-f	IgG1 - 622.3 / 801.5	0.795271353	0.97380276	
M18-g	IgG1 - 622.3 / 654.4	0.636416794	0.914183823	0.899
M18-g	IgG1 - 622.3 / 801.5	0.72214609	0.884261522	
M18-h	IgG1 - 622.3 / 654.4	0.692556696	0.994826244	0.992
M18-h	IgG1 - 622.3 / 801.5	0.807885319	0.989248451	
MF4-a	IgG1 - 622.3 / 654.4	0.656357875	1.000000000	1.000
MF4-a	IgG1 - 622.3 / 801.5	0.74726398	1.000000000	
MF4-b	IgG1 - 622.3 / 654.4	0.612526247	0.933219926	0.948
MF4-b	IgG1 - 622.3 / 801.5	0.719512495	0.962862541	
MF4-c	IgG1 - 622.3 / 654.4	0.630799361	0.961060094	0.946
MF4-c	IgG1 - 622.3 / 801.5	0.696284516	0.931778507	
MF4-d	IgG1 - 622.3 / 654.4	0.604356611	0.920773002	0.929
MF4-d	IgG1 - 622.3 / 801.5	0.701017986	0.938112908	
MF4-e	IgG1 - 622.3 / 654.4	0.611251812	0.931278248	0.939
MF4-e	IgG1 - 622.3 / 801.5	0.707894219	0.947314788	
MF4-f	IgG1 - 622.3 / 654.4	0.610183189	0.929650138	0.927
MF4-f	IgG1 - 622.3 / 801.5	0.691134821	0.924887107	
MF4-g	IgG1 - 622.3 / 654.4	0.621556966	0.946978759	0.943
MF4-g	IgG1 - 622.3 / 801.5	0.702347461	0.939892032	
MF4-h	IgG1 - 622.3 / 654.4	0.590655981	0.899899283	0.911

MF4-h	IgG1 - 622.3 / 801.5	0.689706672	0.922975937	
negA	IgG1 - 622.3 / 654.4	0.768454962	1.000000000	1.000
negA	IgG1 - 622.3 / 801.5	0.894531312	1.000000000	
negB	IgG1 - 622.3 / 654.4	0.724068819	0.942239761	0.951
negB	IgG1 - 622.3 / 801.5	0.85890726	0.960175735	
negC	IgG1 - 622.3 / 654.4	0.67859994	0.883070542	0.886
negC	IgG1 - 622.3 / 801.5	0.795683035	0.889497131	
negD	IgG1 - 622.3 / 654.4	0.726394408	0.945266079	0.942
negD	IgG1 - 622.3 / 801.5	0.839644862	0.938642227	
negE	IgG1 - 622.3 / 654.4	0.69826353	0.908659017	0.924
negE	IgG1 - 622.3 / 801.5	0.840684722	0.93980469	
negF	IgG1 - 622.3 / 654.4	0.715014309	0.930457015	0.928
negF	IgG1 - 622.3 / 801.5	0.827225328	0.924758381	
negG	IgG1 - 622.3 / 654.4	0.746470166	0.971390913	0.965
negG	IgG1 - 622.3 / 801.5	0.857336341	0.958419599	
negH	IgG1 - 622.3 / 654.4	0.74809213	0.973501594	0.962
negH	IgG1 - 622.3 / 801.5	0.850243356	0.950490324	